Haptic Rendering based on Finite Element Simulation of Vibration

Ikumi Susa* Tokyo Institute of Technology
Yukinobu Takehana† Tokyo Institute of Technology
Alfonso Balandra‡ Tokyo Institute of Technology
Hironori Mitake§ Tokyo Institute of Technology
Shoichi Hasegawa¶ Tokyo Institute of Technology / PRESTO, JST

ABSTRACT

Humans can discriminate materials by tapping objects such as metal and wood. When an object is tapped, some natural vibrations occur accordingly to the structure and the physical properties of the object. Humans perceive the natural vibrations through their tactile receptors and then discriminate between materials. In this study, we propose a haptic vibration rendering method based on a finite element vibration simulation. This method allows to display haptic material feelings using 3D models with different shapes and structures.

Keywords: Tapping, vibration haptic rendering, modal analysis.

Index Terms: H.5.2 [Information Interfaces and Presentation]: User Interfaces—Haptic I/O; G.1.8 [Mathematics of Computing]: Partial Differential Equations—Finite element methods

1 INTRODUCTION

When the combination of an event based vibration and feedback forces is rendered in a haptic interface, objects with multiple physical properties such as: shape, stiffness, friction and natural vibration can be presented. The presentation of these physical properties will realize a more realistic haptic interaction.

In this paper, we focus on reproducing the material feeling caused by the object's natural vibrations and shape. The effect when an object is tapped, produces natural vibrations that can heard and felt [6] in addition to static contact forces, all of these are presented in a haptic rendering like virtual couplings.

Humans can discriminate objects' materials only from the vibration in their fingers [8]. When this vibration is rendered in a haptic device, it will realize attractive haptic interactions such as a virtual mock-up with a material sensation.

This paper proposes a haptic rendering method which compute the total presentation force of both natural vibrations and normal forces. Because, the natural vibrations change dynamically depending on the tapping and its positions, our method simulates a corresponding response to the arbitrary user interaction.

2 RELATED WORKS

The presentation of realistic contact by adding vibration through haptic interface has been well investigated in past two decades. Wellman and Howe [13] proposed to present decaying sinusoids vibrations for realistic contacts in a virtual environment. Okamura *et al.* [8] measured and modelled vibrations from taps and strokes to present a haptic vibration for materials and textures. Also Okamura *et al.* [9] proposed to modify the vibration parameters through perceptual experiments with a haptic interface to adjust the limitations of the interface itself. Kuchenbechker *et al.* [7] recorded waveforms with an accelerometer and then played them back with a haptic interface regarding the transfer function between acceleration and force. Their method gives more realism compared with the decayed sinusoids. The approaches above mentioned rely on recording and playback or on mathematical function fittings. Therefore, they do not reproduce the structural vibrations with the corresponding tapping positions.

Sreng *et al.* [11] proposed to present the cantilever beams vibration for impact position discrimination. The Sreng proposal experimented with a physics based model (the Euler-Bernoulli beam) and a simplified model. While the simplified model gives more correlation to impact position, the physics model gives more realism to it. This method employs an analytical solution for a differential equations for a specific shaped objects, so it is not easy to apply to objects with different structure.

Yano *et al.* [14] proposed a finite element model to simulate and generate vibration. However, their method uses the simulation result only to produce sound.

In contrast to the conventional approach, our method uses a numerical simulation to generate the vibrations from objects with an arbitrary structure.

3 PROPOSED METHOD

In this propousal we present the natural vibrations of arbitrary objects, caused by the user's tapping, to give clues about the objects' materials and structures.

Analytical solving methods ,such as [11] formulation, require different equations of motion for every object. In contrast, our method simulates finite element models, whose equations of motion can be intrinsically generated from the structure and the physics parameters of the object. In general, finite element models require a large computation time, and also are difficult to simulate in a haptic refresh rate, while some interactive FEM applications have been proposed [4, 12]. In our method, the displacements caused by the vibrations are small. Therefore, linear analysis is enough and also the realtime computation of the stiffness matrix is not needed. Thus, for small scale finite element models, a realtime simulation is possible.

The natural vibration is caused by external forces. At the time of impact, the finger tip hits the object and gives an impulsive force which generates the vibration. The proposed method simulates dynamics of a finite element model under impulsive forces to compute the waveform of the vibrations. To drive the impedance-type haptic interface, the displacements and velocities of the vibrations are transformed into spring-damper forces, which model the impedance of the finger tip. In addition to vibrations, the normal forces that show the object's shape are presented using a penalty method. Then, at last the the sum of the vibration forces with the penalty method is presented to the user (Fig. 1).

The proposed method calculates the normal forces from feedback loop and the vibration forces from the open loop to eliminate undesirable oscillation; as the same to [9, 7] methods. For the sim-

*e-mail: susa@haselab.net
†e-mail: takehana@haselab.net
‡e-mail: poncho@haselab.net
§e-mail: mitake@haselab.net
¶e-mail: hase@haselab.net

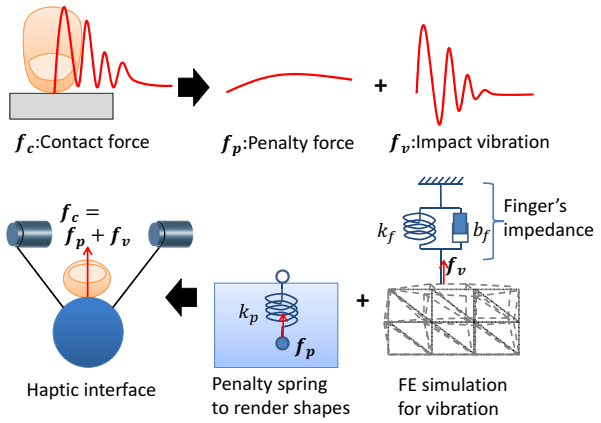

Figure 1: Overview of the proposal

plicity of the simulation model, the proposed system simulates a direct finger-object tapping, while conventional researches deal with a stylus for tapping. The total force f_c presented to the user's finger, via a haptic interface, is the sum of the penalty force $\boldsymbol{f}_p$ and the impact of the vibration force $\boldsymbol{f}_v$. The vibration force $\boldsymbol{f}_v$ is calculated using the finite element model's displacements and velocities and the mechanical model of the user's finger, while the penalty force $\boldsymbol{f}_p$ is calculated with a lower impedance spring and damper model to avoid unstable oscillation.

4 Implementation

This section describes the finite element method vibration simulation and the haptic rendering implementation.

4.1 Object Shape Rendering

The penalty force $\boldsymbol{f}_p$, used to present the object's shape, is calculated from a spring model between the God object [15] and the haptic pointer, whose position immediately reflects the haptic interface's position. The God object's position is updated based on initial object shape and not regarding on the deformation caused by the vibration, because the caused deformation is small and ignorable for the soft spring and also for the penalty force. For the penalty force spring coefficient k_p, the haptic pointer position $\boldsymbol{p}_h$ and the god object position $\boldsymbol{p}_g$, the penalty force $\boldsymbol{f}_p$ is given by

$$\boldsymbol{f}_p = -k_p(\boldsymbol{p}_h - \boldsymbol{p}_g). \tag{1}$$

4.2 Vibration Simulation

This section describes the vibration simulation.

4.2.1 Equation of Motion for Vibration

Because our method employs a finite element method to simulate the vibration [1, 2]. The presented object must be discretized into linear tetrahedron elements, with n total vertices, by using an open source mesh generator named *TetGen*[10]. The global mass matrix $\boldsymbol{M}$, the damping matrix $\boldsymbol{C}$ and the stiffness matrix $\boldsymbol{K}$ are computed using the tetrahedron elements. Then, the equation of motion, of the vertices displacements $\boldsymbol{x} \in R^{3n}$ and external force $\boldsymbol{f} \in R^{3n}$, is given by:

$$\boldsymbol{M}\ddot{\boldsymbol{x}} + \boldsymbol{C}\dot{\boldsymbol{x}} + \boldsymbol{K}\boldsymbol{x} = \boldsymbol{f}. \tag{2}$$

Here, the global damping matrix $\boldsymbol{C}$ is not defined using the material properties, it is defined from tests and identification. So, in this paper, we assume Rayleigh damping, which is often used in vibration analysis. Due to the Rayleigh damping assumption, the global damping matrix is given by:

$$\boldsymbol{C}_{Rayleigh} \equiv \alpha\boldsymbol{M} + \beta\boldsymbol{K} \tag{3}$$

and it is adjusted by modifying $\alpha \in R$ and $\beta \in R$. (This topic will be discussed in detail in section 4.2.2.) In the rest of the paper, we assume $\boldsymbol{C} = \boldsymbol{C}_{Rayleigh}$.

By adding boundary conditions and discretizing the numerical simulation, we can simulate the equation (2) and get the responsive vibration for an arbitrary external force $\boldsymbol{f}$. However, a direct simulation of the equation (2) requires the multiplication of $n \times n$ matrices and n vectors. The order of the computation amount is $O(n^2)$, so a real-time haptic interaction would be difficult to realize because of the large numbers of vertices n. To decrease and limit the computation complexity, this method uses modal analysis to transform the equation (2) into a modal coordinate system. Once the equation (2) is transformed to a set of linear equations with one unknown, the computation complexity is reduced to $O(n)$. Moreover, in modal analysis, the resultant vibration is computed by a superposition of modes, so redundant modes can be omitted. In this paper, the haptic interaction environment for the experiments can't present vibrations more than 300Hz; so we omit modes for more than 300Hz.

To transform the equation (2) into modal coordinates, it is necessary to pre-compute a matrix, called $\boldsymbol{P}$, using the eigenvectors of the global matrix $\boldsymbol{M}$, $\boldsymbol{C}$, $\boldsymbol{K}$. The procedure to get $\boldsymbol{P}$ is mentioned next. For the vibration amplitudes $\boldsymbol{X}$ and the damping natural angular frequency w, the general solution of (2) is obtained as:

$$\boldsymbol{x}(t) = \boldsymbol{X}e^{wt}. \tag{4}$$

By substituting the equation (4) into the equation (2), with $e^{wt} > 0$, we get:

$$(\boldsymbol{M}w^2 + \boldsymbol{C}w + \boldsymbol{K})\boldsymbol{X} = 0. \tag{5}$$

Here, if we assume that $\boldsymbol{C}$ as the Rayleigh damping, then the equation (5) turns to:

$$\left\{(w^2 + \alpha)\boldsymbol{M} + (\beta w + 1)\boldsymbol{K}\right\}\boldsymbol{X} = 0. \tag{6}$$

Then if we define $\Omega^2 = -\frac{w^2+\alpha}{\beta w+1}$ then it transforms into:

$$(-\Omega^2\boldsymbol{M} + \boldsymbol{K})\boldsymbol{X} = 0. \tag{7}$$

where Ω^2 is the eigenvalue (Ω is natural angular frequency of the object without any damping) and $\boldsymbol{X}$ is the respective eigenvector that satisfies the equation (7). Thus, the finding of the matrix $\boldsymbol{P}$ comes from solving the eigenvalues and eigenvectors of $\boldsymbol{M}$ and $\boldsymbol{K}$ with the Rayleigh damping assumption.

For a three dimensional finite element model, the eigenvalues and eigenvectors must have 3 coordinates on every vertex. Thus the matrix $\boldsymbol{P}$ which is defined by the eigenvectors $\boldsymbol{P} = (\boldsymbol{X}_1, \cdots, \boldsymbol{X}_{3n})$, because $\boldsymbol{M}$ and $\boldsymbol{K}$ are symmetric matrices; then their eigenvectors will be orthogonal to each other. Consequently their corresponding eigenvalues will be non zero and different with each other. Then, the eigenvectors $\boldsymbol{X}_1, \cdots, \boldsymbol{X}_{3n}$ are normalized to satisfy $\boldsymbol{P}^T\boldsymbol{M}\boldsymbol{P} = \boldsymbol{I}$. So in this way $\boldsymbol{C}$ and $\boldsymbol{K}$ become:

$$\boldsymbol{C}_m = \boldsymbol{P}^T\boldsymbol{C}\boldsymbol{P} = \begin{pmatrix} \alpha + \beta\Omega_1^2 & & 0 \\ & \ddots & \\ 0 & & \alpha + \beta\Omega_{3n}^2 \end{pmatrix},$$
$$\boldsymbol{K}_m = \boldsymbol{P}^T\boldsymbol{K}\boldsymbol{P} = \begin{pmatrix} \Omega_1^2 & & 0 \\ & \ddots & \\ 0 & & \Omega_{3n}^2 \end{pmatrix}. \tag{8}$$

Next, the equation (2) is transformed into modal coordinates, and the displacement vector $\boldsymbol{x}(t)$ is transformed into the modal displacement vector $\boldsymbol{q}(t)$ as:

$$\boldsymbol{x}(t) = \boldsymbol{P}\boldsymbol{q}(t). \tag{9}$$

Then substituting equation (9) into equation (2), we obtain:

$$\boldsymbol{M}\boldsymbol{P}\ddot{\boldsymbol{q}} + \boldsymbol{C}\boldsymbol{P}\dot{\boldsymbol{q}} + \boldsymbol{K}\boldsymbol{P}\boldsymbol{q} = \boldsymbol{f}. \tag{10}$$

Multiplying $\boldsymbol{P}^T$ on the both sides of the equation (10), and then substituting $\boldsymbol{P}^T\boldsymbol{M}\boldsymbol{P} = \boldsymbol{I}$ from the equation (8); we finally get the equation of motion in modal coordinates as:

$$\ddot{\boldsymbol{q}} + \boldsymbol{C}_m\dot{\boldsymbol{q}} + \boldsymbol{K}_m\boldsymbol{q} = \boldsymbol{P}^T\boldsymbol{f}. \tag{11}$$

Because $\boldsymbol{C}_m$ and $\boldsymbol{K}_m$ are diagonal matrices, the equation (11) will be independent linear equations.

The responsive vibration is obtained by simulating the equation (11) considering the boundary conditions and the contact impulse in realtime. For the numerical integration, a Newmark-beta method, with $\beta = 1/4$, is used to make the numerical integration implicit and stable. The updated displacements $\boldsymbol{x}(t+\delta t)$ and velocities $\dot{\boldsymbol{x}}(t+\delta t)$ of the tetrahedra vertices in the finite element model can be obtained by substituting the modal displacement vector $\boldsymbol{q}(t+\delta t)$ and the modal velocity vector $\dot{\boldsymbol{q}}(t+\delta t)$ into the equation (9).

4.2.2 Rayleigh Damping

In this section, the method to find Rayleigh damping coefficients, α and β, will be discussed.

As mentioned in the previous section, the Rayleigh damping is defined by the equation (3), while in modal analysis the Rayleigh damping decays for each modal vibration, as shown in the equation (8). This damping factor is represented by a damping ratio ζ_i, for the i-th natural vibration mode; the damping ratio is given by:

$$\zeta_i = \frac{1}{2}(\frac{\alpha}{\Omega_i} + \beta\Omega_i). \tag{12}$$

For the damping ratio $\zeta_i \geq 1$, the i-th natural mode stops vibration and makes an aperiodic motion instead. On the other hand, for $\zeta_i < 1$, the i-th natural mode vibrates with a slow convergence. In addition, for ζ_i near to 1, the damping is strong with a fast convergence, while for ζ_i near to 0, the damping is weak and the vibration remains for a longer period.

The Rayleigh damping coefficients, α and β, can be found by setting the damping ratios for multiple natural modes and solving multiple simultaneous equations (12) with a direct method or least squares method. To replicate the vibration phenomena on a real object, it is necessary to find the damping ratios from the test results and identification of coefficients are needed.

In our implementation, we compute the coefficients α and β by setting the 1st natural mode damping ratio m_1 in the smallest vibration frequency and the m th natural mode in the largest frequency. Then the equation (12) is solved simultaneously as:

$$\begin{aligned}\alpha &= \frac{2\Omega_1\Omega_m}{\Omega_m^2 - \Omega_1^2}(\Omega_m\zeta_1 - \Omega_1\zeta_m),\\ \beta &= \frac{2\Omega_1\Omega_m}{\Omega_m^2 - \Omega_1^2}(\frac{\zeta_m}{\Omega_1} - \frac{\zeta_1}{\Omega_m}).\end{aligned} \tag{13}$$

4.3 Impact force calculation

When the haptic pointer contacts the object, the impact impulse is applied to the corresponding vertices of the finite element model. The impact impulse $\boldsymbol{p}$ is calculated applying the normal component of the finger momentum:

$$\boldsymbol{p} = -m(\boldsymbol{n}\cdot\boldsymbol{v})\boldsymbol{n}. \tag{14}$$

Where, $\boldsymbol{n}$ is the surface normal, $\boldsymbol{v}$ is the relative finger velocity just before the contact and m is the mass of the finger.

Next, the impulse $\boldsymbol{p}$ is distributed within the tetrahedron vertices in contact with the haptic pointer. From the contact position (*i.e.* God object's position on the contact surface), a contact tetrahedron element is found. Then, the impact impulse force $\boldsymbol{p}$ is distributed using a shape function of the element regarding the God object's position $\boldsymbol{r}_g$ and the initial position of the element; as shown here:

$$\boldsymbol{p}_i = \boldsymbol{p}N_i(\boldsymbol{r}_g) \tag{15}$$

where N_i is the shape function and $i \in 1, 2, 3, 4$. Then, the distributed impulsive forces $\boldsymbol{p}_i$ are transformed into modal coordinates and applied to the vibration simulation based on the equation (11), taking the simulation time step period into account.

4.4 Vibration Haptic Rendering

The vibration force $\boldsymbol{f}_v$ is calculated from the vibration at the contact position (*i.e.* God object's position). The vibration in the contact position is calculated using the tetrahedron element's shape functions. These calculations ignore the vibration displacements, because are based on the tetrahedra initial state. So, the contact point displacement $\boldsymbol{x}_c$ and velocity $\dot{\boldsymbol{x}}_c$ are given as:

$$\boldsymbol{x}_c = \sum_{i=1}^{4} = N_i(\boldsymbol{r}_g)\boldsymbol{x}_i, \quad \dot{\boldsymbol{x}}_c = \sum_{i=1}^{4} = N_i(\boldsymbol{r}_g)\dot{\boldsymbol{x}}_i, \tag{16}$$

Where, $\boldsymbol{x}_i$ is the i vertex displacement, $\dot{\boldsymbol{x}}_i$ is the i vertex velocity and i is contact vertex of the tetrahedron element. Finally, the presenting vibration force $\boldsymbol{f}_v$ can be written as:

$$\boldsymbol{f}_v = (k_f(\boldsymbol{x}_c\cdot\boldsymbol{n}) + b_f(\dot{\boldsymbol{x}}_c\cdot\boldsymbol{n}))\boldsymbol{n} \tag{17}$$

with the spring and damping coefficient k_f and k_v respectively and the contact surface normal $\boldsymbol{n}$. For k_f and k_v, representative finger's values of 300N/m and 3Ns/m are used, referring to [3].

4.5 Combination of Penalty Force with Natural Vibration

The feedback force presented in the haptic interface consist of the sum of the penalty forces, mentioned in section 4.1, and the natural vibration force mentioned in section 4.4. At the end, the result force $\boldsymbol{f}_c$ is calculated as:

$$\boldsymbol{f}_c = \boldsymbol{f}_p + \boldsymbol{f}_v. \tag{18}$$

5 Evaluation

For the evaluation, a haptic interaction environment was set up with a PC (Windows 7, Intel(R) Core(TM) i7-2640M CPU 2.8GHz) and the haptic interface SPIDAR-G6 whose characteristics were evaluated in [5]. The haptic interface can present vibration of up to 300Hz. We choose a grip type device instead of a finger cap type device to avoid giving an stress force to the finger before the contact impact. We ask the users to put their index finger on the grip and grasp it by the thumb and the middle finger as shown in Figure 6.

In the vibration simulation, the penalty force rendering and the vibration force are computed in a different thread with a 1ms update rate; through a Windows API multimedia timer. And also the graphics are rendered in another thread. Any parallel computing devices or special hardware had not been used. Figure 2 shows the finite element model for experiments, this image shows the finite element model vertices and edges.

At the begining, for the finger mass value, in section 4.3, we try to use a mass of 5.8g as a value taking from [3]. However, when users tap virtual plates, the presented vibrations are far smaller than tapping vibration in the real world. Therefore, we use a mass of 58g which includes the inertia of the haptic interface. With this value,

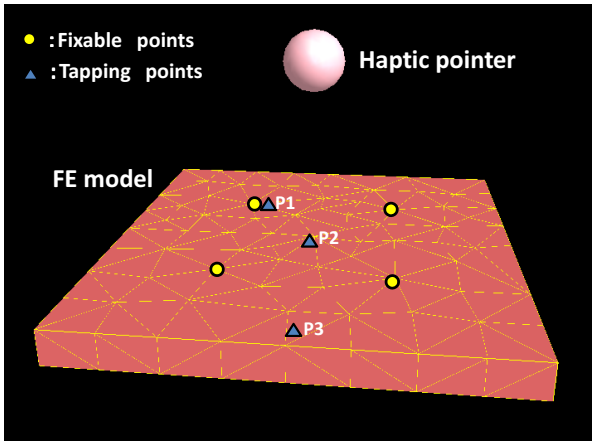

Figure 2: The finite element model and the boundary conditions

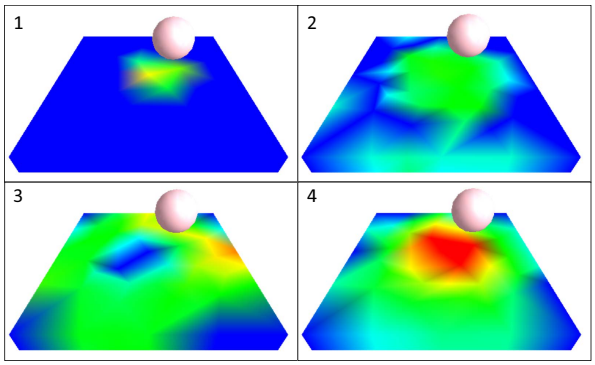

Figure 3: Visualization of the vibration

the users' felling vibration of virtual plates is similar to their real plates perception.

Figure 3 shows a visualization of the implemented simulator. Here, four bottom corners of the model are fixed. The images are a transition of vibration displacements. The blue and red colors represent small and large displacements respectively.

5.1 Haptic Rendering Output Force

To confirm the appropriateness of the rendering and the simulation, we recorded the feedback forces during haptic interaction. During the recording, a plate model shown in Figure 3 is fixed in two or four points and then tapped by users, where the tapping points are P1,P2 and P3. To reproduce a boundary condition of a real plate fixed by screws, both the top and bottom sides vertices are fixed for each fixed point. Therefore, the number of the fixed vertices are four and eight respectively.

Table 1 shows the plate model's parameters, except for damping ratio, all the material parameters are based on aluminium, acrylic and MDF's physical properties.

The plate models are fixed by four bottom corner vertices that have 267 modes and the vibration is simulated by 55 modes, whose natural vibration frequencies are between 0-300Hz. For the damping matrix $\boldsymbol{C}$ we set the damping ratio, with lowest natural vibration frequency ζ_1 and highest natural vibration frequency ζ_{55}, comparing the resultant simulation form and the real tapping wave form. Then, we compute the coefficients α and β by the method described in section 4.2.2. This coefficients α and β are used to calculate the damping matrix $\boldsymbol{C}$ for all following simulation, ignoring the numbers and the positions of the fixed points. The spring coefficient of the penalty force for shape rendering is adjusted to 3000 N/m to provide stability. The computation time for the modal simulation is less than 0.22ms with an average of 0.18ms. In consequence, the update rate of the haptic loop can be kept in 1ms.

Table 1: Parameters of the plate model

Plate size		$0.6 \times 0.6 \times 0.05$ m
Number of tetrahedrons		443
MDF	Young's modulus	2.5 GPa
	Density	$0.61 \times 10^3 \mathrm{kg/m^3}$
	Poisson's ratio	0.250
	Rayleigh Coefficient	α: 120.0 , β: 7.05×10^{-5}
Acrylic	Young's modulus	3.2 GPa
	Density	$1.18 \times 10^3 \mathrm{kg/m^3}$
	Poisson's ratio	0.350
	Rayleigh Coefficient	α: 120.0 , β: 8.50×10^{-5}
Aluminum	Young's modulus	1.0 GPa
	Density	$2.70 \times 10^3 \mathrm{kg/m^3}$
	Poisson's ratio	0.345
	Rayleigh Coefficient	α: 100.8 , β: 1.50×10^{-5}

Figure 4 and Figure 5 show feedback forces when user tapped P1,P2 and P3. Figure 4 shows the feedback forces under two points fixation, while Figure 5 shows the feedback forces under four fixation points. When the user taps on P1, which is near to a fixed point, with two or four fixed points; almost all the feedback force consists on the penalty forces and no vibration is observed. When the user taps on P2, which is placed at the center of the plate, low frequency modes excitations are not observed, while the vibrations corresponding to high frequency modes are well observed especially in aluminum case. When the user taps on P3, in the MDF and acrylic plates, large vibrations corresponding to the low frequency modes are observed in two fixed points case. While for the aluminium vibration is smaller; reflecting a larger Young's modulus. In the four fixed point case, P3 is near to the fixed points, so the vibrations corresponding to the low frequency modes can not be observed well.

From the results above, we consider that the feedback vibrations of the proposed method reflect the material and structure of the tapped objects.

5.2 User study

To confirm the effect of the proposed simulation, two user studies were conducted; one for evaluating the haptic rendering of the tapping vibration in the structure and the material discrimination, and the other for the reality assessment.

5.2.1 Structure and material discrimination

As shown in Figure 6, we fixed the acrylic and the MDF plate on a iron block or a plate with two and three fixation points. Both, the iron block and the plate were very heavy, so the excitations of vibration modes were far smaller compared to the acrylic and MDF plates. The haptic interface Spidar G6 was also used to present the virtual plates.

In the experiment, the users can freely tap the virtual plate, presented in the haptic interface, and the four real plates. Then the users are asked which real plate is the most similar to the virtual plate.

During the experiment, the user can see the 3D solid model of the plate and the haptic pointer in a normal monitor. Then, to eliminate any clue from visual and sound channel, the graphics do not reflect

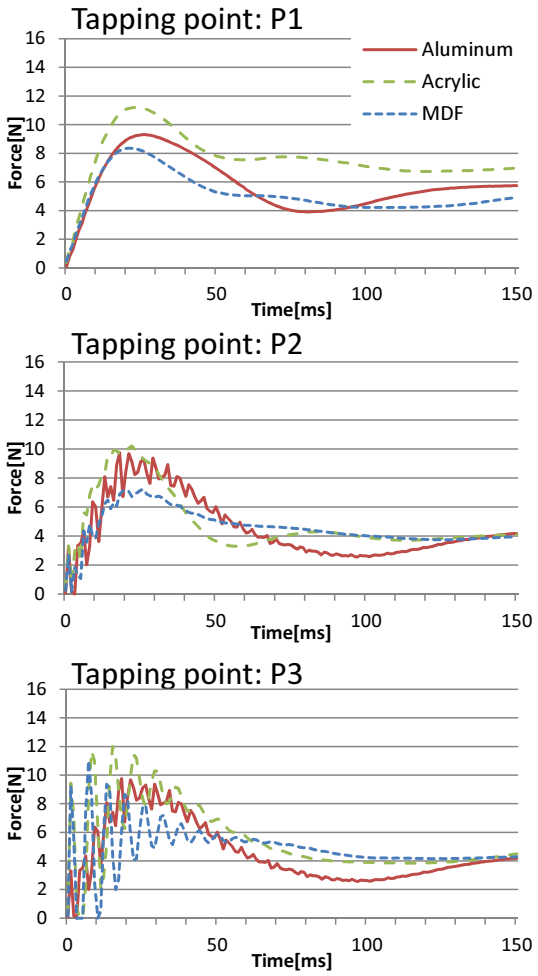

Figure 4: Feedback force of penalty and vibration; Two points fixation

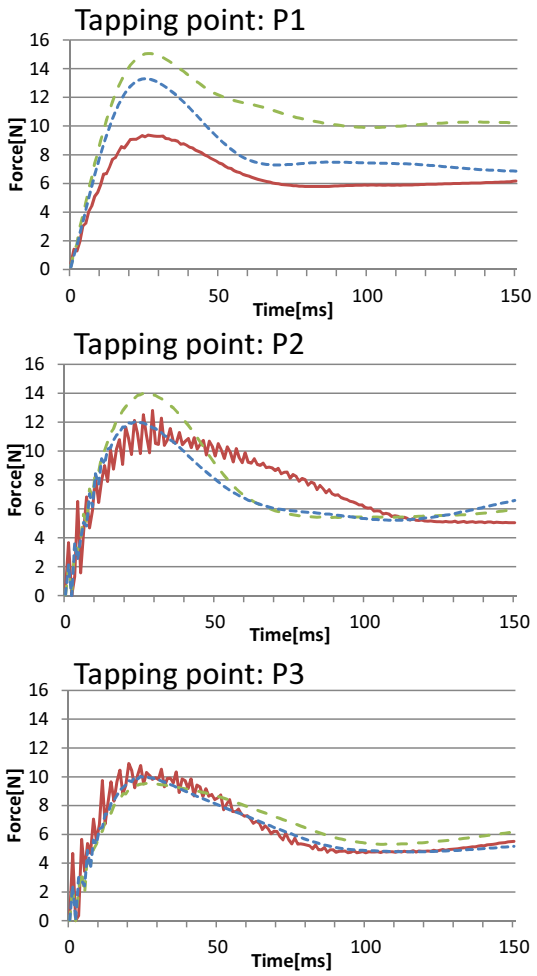

Figure 5: Feedback force of penalty and vibration; Four points fixation

Table 2: Confusion matrix for the structure and material discrimination experiment

Answer / Display	Acrylic two fix	MDF two fix	Acrylic three fix	MDF three fix
Acrylic two fix	10	5	2	3
MDF two fix	7	10	3	0
Acrylic three fix	1	3	11	5
MDF three fix	1	2	5	12

the plate's material or the plate vibration and users can just hear white noise through in-ear headphones, while they wear acoustic earmuffs. The physical parameters of the acrylic and MDF plates are the same to the ones shown in Table 1. Ten males, in their twenties, participate in the experiment. Four virtual plates whose parameters are same to the four real plates are presented. Each one of the plates are presented twice with a randomized presentation order.

Table 2 shows the resultant confusion matrix of the experiment. Most participants could discriminate the plate structure well, while only the 2/3 answers are correct for material discrimination.

5.2.2 Reality assessment

For reality assessment, the four participants are asked to answer which is the most realistic virtual plate from three types of haptic

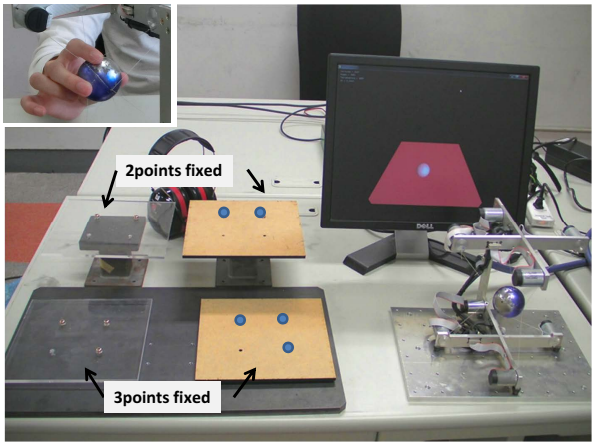

Figure 6: The Evaluation System and The Grasp Manner

rendering techniques: no vibration, the event based decayed sinusoid regarding [8] and the proposed finite element simulation based rendering.

During the experiment, the user can freely tap the real acrylic and

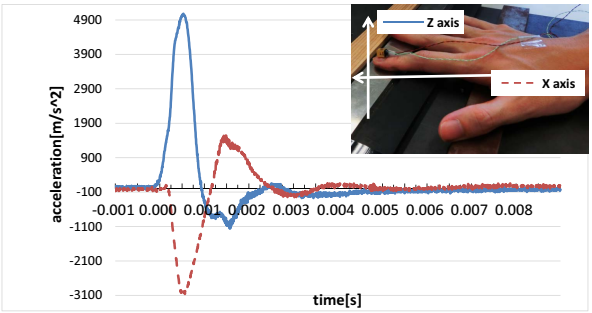

Figure 7: Accelerometer on finger and the tapping finger acceleration

the MDF plate. Then the researcher switches the rendering technique between the three possible options. In case the participants ask to try any one of the three options, the researcher responds to the request.

As a result, all four participants chose the proposed technique as most realistic one.

5.2.3 Effect of finger vibration

Some users report that the tapping feel on P1 is too soft and is not very realistic. Therefore, we measure the vibrations with fixed plate and the user's finger.

We attach an accelerometer (*35A* from *ENDEVCO*) on the user's index fingernail using quick drying glue, where the weight of the accelerometer is small (1.1g). Figure 7 shows the measured acceleration of one tapping Also the vibrations of the tapped plate were measured by attaching the accelerometer near to the tapped position. In addition, we measure the vibrations using a laser displacement meter (*LK-G30* from *KEYENCE*) to confirm the order of the vibration. It was confirmed, that the vibration of the plate is at least 100 times smaller than the finger's vibration.

The measured finger acceleration in Figure 7 changes very fast, so it can not be reproduced by our haptic environment. Instead, we add a two times slower decayed sinusoid $Ae^{-600t}\sin(250 \cdot 2\pi t)$, where the amplitude A is proportional to the tapping velocity and the coefficients where found by cut and try.

Finally, we conduct a reality assessment again. The setup was the same to the previous experiment in section 5.2.2. But this time, we show three different types of haptic rendering techniques: the simulation based rendering, the decayed sinusoid and simulation based rendering with the decayed sinusoid. Ten users participate in the experiment, and seven of them choose the simulation based rendering with decayed sinusoid, as the most realistic one, which considers the finger vibration. The remaining three participants choose the simulation based rendering.

6 Conclusion

In this paper, we presented a vibration rendering based on realtime finite element modal simulation for an arbitrary object structure and material. We confirmed that the output forces after tapping reflect both the structure and the material of the tapped objects. Also, we conducted two user studies, the first one suggests that users can discriminate between structures and materials, and second one shows that the proposed method presented the most realistic vibration.

7 Limitations and Future Work

This paper deals with vibration of just one object tapped by just one finger. The vibration from two or more contacting-objects requires further research. In addition, the modal simulation does not consider the effect of the contact or vibration on the finger. As future work we consider to work on a multi-softbody simulator, which considers the user's fingers vibration.

In the evaluation, we used 10 times larger mass for the impact force calculation to produce realistic vibrations. The velocities of the haptic pointer were around three times slower than the real tappings. So, the impact momentum of the virtual finger would be around three times larger than the real one and there would be other reason to make the vibration's feeling small.

References

[1] R. Cook, D. Malkus, R. Witt, and M. Plesha. *Concepts and Applications of Finite Element Analysis*. John Wiley and Sons, Inc., 4th edition edition, 2007.

[2] Z. Fu and J. He. *Modal Analysis*. Elsevier Science, 2001.

[3] A. Z. Hajian and R. D. Howe. Identification of the mechanical impedance at the human finger tip. *Journal of Biomechanical Engineering*, 119(1):109–114, 1997.

[4] K. K. Hauser, C. Shen, and J. F. O'Brien. Interactive deformation using modal analysis with constraints. In *Graphics Interface*, pages 247–256. CIPS, Canadian Human-Computer Commnication Society, jun 2003.

[5] Y. Ikeda and S. Hasegawa. Short paper: Characteristics of perception of stiffness by varied tapping velocity and penetration in using event-based haptic. *Joint Virtual Reality Conference EGVE-ICAT-EURO VR*, pages 113–116, 2009.

[6] R. S. Johansson et al. Responses of mechanoreceptive afferent units in the glabrous skin of the human hand to sinusoidal skin displacements. *Brain research*, 244(1):17–25, 1982.

[7] K. J. Kuchenbecker, J. Fiene, and G. Niemeyer. Improving contact realism through event-based haptic feedback. *IEEE Transactions on Visualization and Computer Graphics*, 12(2):219–230, 2006.

[8] A. Okamura, J. Dennerlein, and R. Howe. Vibration feedback models for virtual environments. In *Robotics and Automation, 1998. Proceedings. 1998 IEEE International Conference on*, volume 1, pages 674–679 vol.1, 1998.

[9] A. M. Okamura, M. R. Cutkosky, and J. T. Dennerlein. Reality-based models for vibration feedback in virtual environments. *IEEE/ASME Transactions on Mechatronics*, 6, Issue: 3:245–252, 2001.

[10] H. Si and A. TetGen. A quality tetrahedral mesh generator and three-dimensional delaunay triangulator. *Weierstrass Institute for Applied Analysis and Stochastic, Berlin, Germany*, 2006.

[11] J. Sreng, A. Lécuyer, and C. Andriot. Using vibration patterns to provide impact position information in haptic manipulation of virtual objects. In *Proceedings of the 6th international conference on Haptics: Perception, Devices and Scenarios*, EuroHaptics '08, pages 589–598, Berlin, Heidelberg, 2008. Springer-Verlag.

[12] N. Umetani, J. Mitani, T. Igarashi, and K. Takayama. Designing custommade metallophone with concurrent eigenanalysis. In *New Interfaces for Musical Expression++ (NIME++)*, pages 26–30, 2010.

[13] P. Wellman and R. D. Howe. Towards realistic vibrotactile display in virtual environments. In *Proceeding of the ASME Dynamics Sys. and Control Division, Symposium on Haptic Interfaces for Virtual Environment and Teleoperator Sys., Alberts T. ed*, pages 57–2, 1995.

[14] H. Yano and H. Iwata. Software architecture for audio and haptic rendering based on a physical model. In *Proceedings of the 8th IFIP TC13 conference on human–computer interaction, Tokyo, Japan*, pages 19–26, 2001.

[15] C. B. Zilles and J. Salisbury. A constraint-based god-object method for haptic display. In *Intelligent Robots and Systems 95. 'Human Robot Interaction and Cooperative Robots', Proceedings. 1995 IEEE/RSJ International Conference on*, volume 3, pages 146–151 vol.3, 1995.